

NUMERICAL MODELING OF TEMPERATURE DISTRIBUTION IN LASER BEAM WELDING OF 304 STAINLESS STEEL

PRAMOD KUMAR¹ & AMAR NATH SINHA²

¹Research Scholar, Department of Mechanical Engineering, National Institute of Technology, Patna, India

²Associate Professor, Department of Mechanical Engineering, National Institute of Technology, Patna, India

ABSTRACT

A numerical method for solving the laser welding problem of heating and melting is developed in the present investigation. Laser welding is a fast, unbalanced and complex process which requires a non-uniform heat transfer analysis. A three-dimensional Gaussian heat distribution equation for moving heat source with conical shape has been incorporated in this present model. A finite element code using software ANSYS has been developed which takes into account the thermal and mechanical aspect of the material. Properties of the material AISI 304 austenitic stainless steel are taken as temperature dependent in this simulation, which has great influence on the temperature profile. The effect of laser beam power, welding speed, spot radius and mesh density on temperature profile, bead geometry, and shape of the molten pool has been studied. The geometry created for this model is similar to the butt-joint of 2.5mm thick material and cooling effect caused by the free convection and radiation in ambient air is taken into account. The shape of the molten pool obtained from the numerical simulation was in good agreement with the published result.

KEYWORDS: Laser Welding, Numerical Simulation, Butt-Joint, Temperature Profile, FEM & ANSYS

Received: Mar 20, 2018; **Accepted:** Apr 10, 2018; **Published:** May 10, 2018; **Paper Id.:** IJMPERDJUN201850

INTRODUCTION

Laser welding technique is a widely growing technology in today's era due to its very smooth, precise and effective operation. It has a major advantage over the other welding techniques is that it is a very quick process and comparatively very less heat affected zone and distortion are generated and automation can be easily done. Laser welding is a fast and complex process in which phase transformation, energy absorption, and reflection occur simultaneously. Many of the numerical simulation models have been developed using finite element method to predict temperature distribution, stress and distortion in the welded joint. Large numbers of experimental trials were done before to optimize the laser welding parameter which was not economical and time-consuming. Finite element numerical simulation has been an evolution in the welding processes area as these numerical methods can be used efficiently to optimize the laser welding process parameters.

Laser welding is finding a numerous application in different areas like industry, medical, automotive etc. This technique is finding a wide range of application as it has great advantages over other welding techniques like it can be easily automated, narrow heat affected zone and minimum distortion and high accuracy and precision. In recent years the use of laser welding in the automotive industry is increasing dramatically. Many researchers have been working in the area of numerical modeling of laser welding for determining the temperature distribution and weld bead geometry. The analytical solution of the PDE for applying the moving heat source was proposed by Rosenthal [1] which was simplified as a moving point heat source in numerical simulation. Frewin and Scott [2]

used a finite element model of the heat flow during pulsed laser beam welding. They have calculated transient temperature profiles and the dimensions of fusion zone and HAZ. Tsirkas et al. [3] Studied the numerical simulation of the laser welding process for determining the distortion in the welded joint using SYSWELD software package and the results was experimentally validated with good agreement. Guoming et al. [4] have studied the temperature distribution in laser welding of stainless steel 304Lis used ANSYS simulation software and predicted the weld shape of the welded joint and compared with the experimental results. Spina et al. [5] have predicted the induced distortions in thin plates and T-joints of aluminum alloys and observed that a correct thermal analysis is mandatory to predict welding induced distortions and residual stresses in laser beam welding of AA5083 alloys. For deeper penetration welding, the volumetric heat source with a Gaussian conical profile of the laser beam is used. These analytical and numerical models are based on the heat conduction-based models. Studies showed that the laser welding process is very complex because the weld pool geometry is influenced by both heat transfer and fluid flow in the fusion zone [6]. Laser welding of 304 stainless steel of 2.5mm thickness and finite element modeling of temperature field was investigated by Shanmugam et al. [5]. They indicated that the distance between the center of the laser beam spot and the location where the peak temperature occurred increased slightly as the laser power was increased; however, the opposite was true when the welding speed was decreased. Akman et al. [8] Have studied the welding of Ti6Al4V titanium alloys using pulsed Nd: YAG laser welding method was done by They have observed that it was possible to control the penetration depth and geometry of the laser weld bead by precisely controlling the laser output parameters. Kim, K. et al. have studied the pulsed welding with Nd:YAG laser applied for joining austenitic CrNi steel type AISI 304, 1, 2 and 3 mm in thickness. Numerical simulation was done in a program based on the finite-element method [8]. Some studies that involve liquid motion around the keyhole have also been reported by Wang. et al.[10]. Few numerical modeling studies involving fluid flow by tracking the keyhole surface have also been reported. Casalino et al. [12] predicted the temperature history during the laser welding process through finite element modeling. They have also compared the numerical results with experimental values. Chukkan et al. [13] have studied the temperature profile using FEM and observed that it had higher accuracy than simplified mathematical model because of the consideration of the heterogeneous heat source, the nonlinear material properties, and the heat exchange with the environment. K Suresh Kumar [14] has studied the pulsed butt laser welding of 316L stainless steel of 2mm thickness using finite element method COMSOL software package. The incident laser beam was numerically modeled as a rectangular pulsed Hermit-Gaussian heat source and distributed spatially at TEM00 mode. He predicted the transient thermal responses across the weld joint and along the penetration depth and maximum/minimum temperatures were also measured during laser welding.

The present work aims to study the temperature profile and shape of the weld bead, molten zone and the effect of process parameters such as laser power, welding speed and spot radius on temperature profile and molten pool shape in laser welding using finite element code ANSYS. The material used for this work is AISI 304 austenitic stainless steel thickness 2.5mm and the physical properties of the material (density, thermal conductivity, and specific heat) are considered as temperature dependent. A three-dimensional Gaussian moving heat source with conical shape has been employed in this work. The temperature profile, peak temperature, shape of molten pool and weld bead are then compared with the results of published papers for same process parameters.

HEAT TRANSFER ANALYSIS

It is desirable to find the effect of laser welding process parameters on the temperature field formed due to irradiation of the laser if we want to find the relation between molten pool shape and welding parameters. The basic governing equation of the three-dimensional heat conduction for transient temperature is given as in equation 1[3].

$$\rho c \frac{\partial T}{\partial \tau} + v \rho c \frac{\partial T}{\partial y} = \frac{\partial}{\partial x} \left(K_x \frac{\partial T}{\partial x} \right) + \frac{\partial}{\partial y} \left(K_y \frac{\partial T}{\partial y} \right) + \frac{\partial}{\partial z} \left(K_z \frac{\partial T}{\partial z} \right) + Q \quad (1)$$

Where T is the temperature ($^{\circ}\text{C}$) which is a function of time and space, ρ is the density of the material (kg/mm^3), c is the specific heat of the material ($\text{J/kg}^{\circ}\text{C}$), v is the laser scanning speed or welding speed (mm/s), k is the thermal conductivity of the material ($\text{W/mm}^{\circ}\text{C}$) and Q is the heat source, expressed as heat generation per unit volume (J/mm^3). It has been assumed that laser beam follows the Gaussian heat source distribution of conical shape moving with velocity v along the y -axis.

HEAT SOURCE MODELING

It has been found experimentally that 30.7% of the total power is lost and rest 69.3% power is absorbed by the work piece in case of AISI 304 stainless austenitic stainless steel [3]. For simulation, it has been considered that the heat source is a combination of a plane heat source distributed on the top surface and a conical heat source distributed along the thickness of material (figure. 1). It is assumed that about 69.3% of total power, 17.3% power is absorbed on the top surface (Q_{surf}) and rest 52% power is distributed in the material in conical shape (Q_{keyhole}). Figure 1 represents the distribution of the heat on the surface and along the thickness.

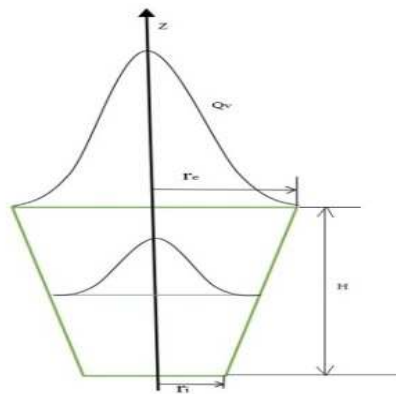


Figure 1: Conical Gaussian Heat Source Model

The distribution of heat on the top surface is given as in equation 2.

$$Q(x, y) = \frac{3Q_{\text{surf}}}{\pi R^2} e^{\left(-\frac{3(x^2 + (y - vx)^2)}{R^2} \right)} \quad (2)$$

Where, Q_{surf} is the heating power of the plane heat source (17.3%) and R is the radius of heat source. It has been assumed the simulation of keyhole is a cone, the Gaussian distribution of heat flux is given as in equation 3.

$$Q(z) = \frac{2Q_{keyhole}}{\pi r_o^2 H} e^{-1 - \left(\frac{x^2 + (y-vx)^2}{r_o^2} \right)} \left(1 - \frac{z}{H} \right) \quad (3)$$

Where, $Q_{keyhole}$ is the absorbed laser power (52%), H is the sheet thickness, r is the current radius, z is the current depth and r_o is given as in equation 4.

$$r_o = r_e - (r_e - r_i) \left(\frac{z_e - z}{z_e - z_i} \right) \quad (4)$$

Where, z_e and z_i are the z -coordinates at the top and bottom surface respectively. r_e and r_i are the radius at the top and bottom surface respectively. The total heat input given to the model is the combination of both surface and volume heat source models, which can be expressed as given in equation 5.

$$Q_v(r, z) = Q(x, y) + Q(z) \quad (5)$$

MATERIAL AND METHOD

The material considered for this project work is AISI 304 austenitic stainless steel of thickness 2.5mm. The chemical composition of the material is given in table I. The thermo-physical properties of this material are taken as temperature dependent which is given in Table 2. The melting and vaporization temperature of this material is 1450 °C and 2467 °C respectively.

Table 1: Chemical Composition of AISI 304 Stainless Steel in Weight Percentage [7]

C	Cr	Fe	Mn	P	S	Si	Ni
0.055	18.28	66.34	1.00	0.029	0.005	0.6	8.48

Many process parameters are there in laser welding which affect the peak temperature, temperature profile and molten pool shape. The welding parameters such as beam power, welding speed and spot diameter chosen for this research are given in Table 3.

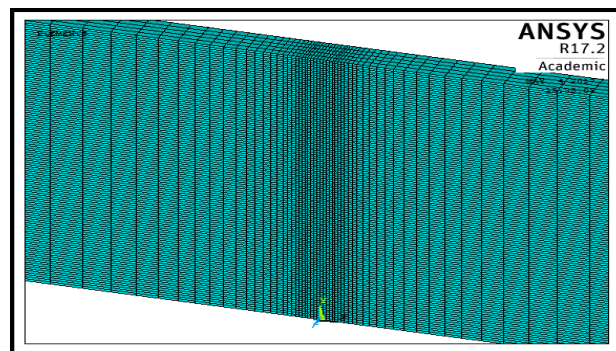
Table 2: Material Properties of AISI 304 Stainless Steel [11]

Temperature (°C)	Thermal Conductivity (W/m·°C)	Specific Heat (J/kg·°C)	Density (kg/m ³)
0	14.6	496	7900
100	15.1	512	7880
200	16.1	525	7830
300	17.9	540	7790
400	18	577	7750
600	20.8	604	7660
800	23.9	676	7560
1200	32.2	692	7370
1300	33.7	700	7320
1500	120	496	7320

Table 3: Laser Welding Parameters

Sl. No	Beam Power (Watt)	Welding Speed (mm/min)	Spot Diameter (mm)
1	1000	400	0.6
2	1400	400	0.6
3	1800	400	0.6
4	1000	800	0.6
5	1400	800	0.6
6	1800	800	0.6
7	1000	400	0.8
8	1400	400	0.8
9	1800	400	0.8
10	1000	800	0.8
11	1400	800	0.8
12	1800	800	0.8

A three dimensional finite element model has been developed to simulate the laser welding process using commercial software ANSYS. The geometry of the one plate in a butt joint taken for the modeling is 25mm X 25mm X 2.5mm. The model developed is used to predict the temperature profile, molten pool shape and peak temperature and the effect of laser parameters. The geometry of the weld structure is modeled using two types of elements: SOLID 70 and PLANE 55. A finite element mesh of the geometry is shown in figure. 2.

**Figure 2: Mesh of the Geometry**

The meshing is done in such a way that a very fine mesh will be there near the weld line and size of the meshing becomes coarser as the distance from the weld line increases in either direction. There are total 46494 nodes and 43500 elements in full part of the model. A number of convergence test has been done for 6,8,10 elements across the weld line and 4,5,6 elements along thickness to get the accurate result and it comes out that 8 elements across the weld line and 5 elements along the thickness gives the most accurate result. There are certain assumptions made for this project work.

- The initial temperature of the workpiece is taken as 30°C.
- Thermo physical properties of the material such as density, specific heat, thermal conductivity are taken as temperature dependent.
- Radiation and convection heat loss from the surfaces of the workpiece are taken into account.

SIMULATED RESULTS AND DISCUSSIONS

A finite element model is developed using the finite element code ANSYS to study the temperature profile and shape of molten pool. The number of simulations has been done for different welding parameters and the effect of these parameters on temperature distribution and shape and size of molten pool has been studied. The parameters used for this project work are listed in Table 3. The results obtained in this project work are then compared with the results from a published paper [3] for same welding parameters. The shape and size of the molten pool are predicted from the melting (1450°C) and vaporization (2467°C) isotherms.

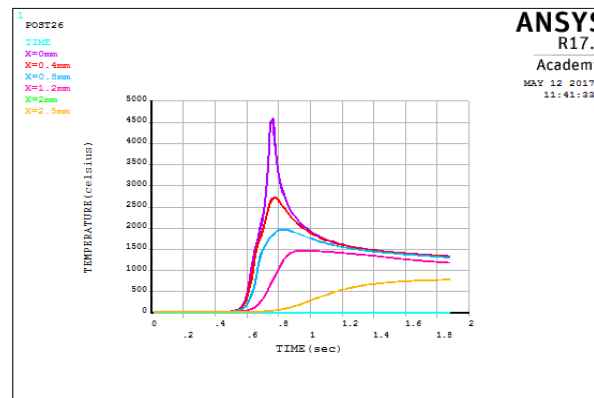


**Figure 3(a): Temperature Distribution across Weld Axis
Beam Power 1800W, Welding Speed 800mm/min,
0.8 mm Spot Diameters**

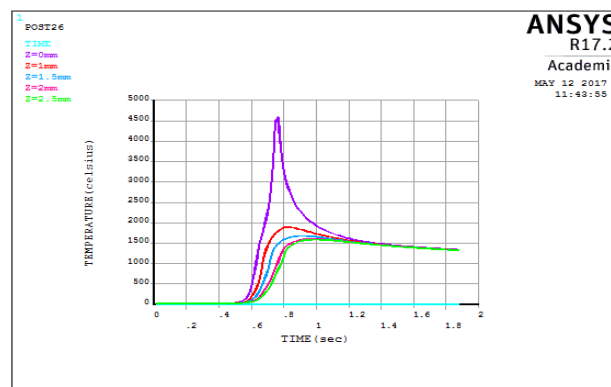


**Figure 4(b): Temperature Distribution along Thickness at Load
Step 50, Beam Power 1800W, Welding Speed 800mm/min,
0.8 mm Spot Diameters**

Figure 3 represents the temperature distribution for 1800W beam power, 800mm/min welding speed and 0.8mm spot diameter in both the directions, across the weld line and along the thickness. Figure 3 (a) shows the variation of power across the weld line and it clearly shows that the temperature is decreasing rapidly as we move away from the weld line and decreases up to nearly 800°C at 2.5mm from the weld line. The maximum value of peak temperature (4613°C) occurs along the weld line which is more than the vaporization temperature of the material. Figure 3 (b) shows the variation of the temperature profile along the thickness and it can be concluded that the temperature decreases very rapidly for the first half and then it decreases gradually for the second half. The temperature at the bottom surface is more than 1500°C which is greater than the melting temperature, which shows that full penetration occurs for these welding parameters.

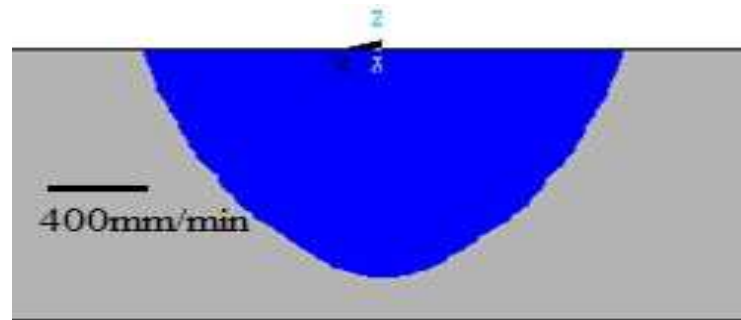


Figure 5(a): Effect of Welding Speed on Bead Geometry For Welding Parameters 1000W Beam Power, 0.8mm Spot Diameter Welding Speed 400mm/min

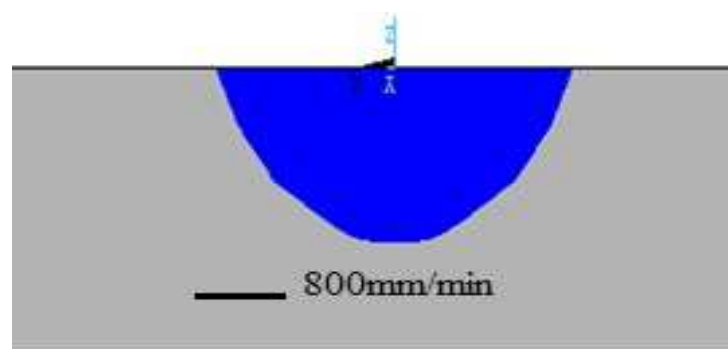


Figure 6(b): Effect of Welding Speed on Bead Geometry For Welding Parameters 1000W Beam Power, 0.8mm Spot Diameter Welding Speed 800mm/min

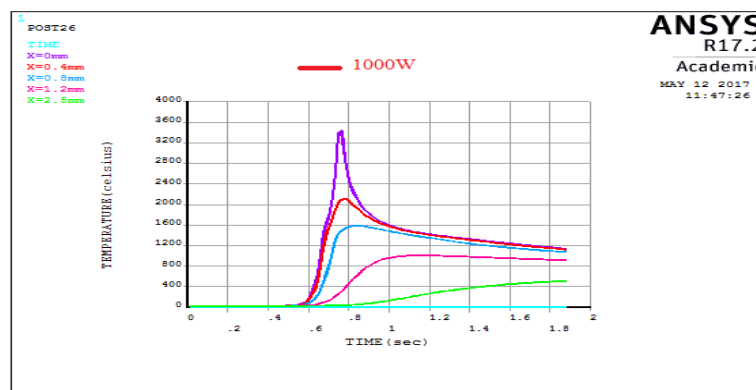


Figure 7(a): Effect of Beam Power on Temp Distribution for the Laser Parameters 800mm/min Welding Speed and 0.8mm Spot Diameter Beam Power 1000W

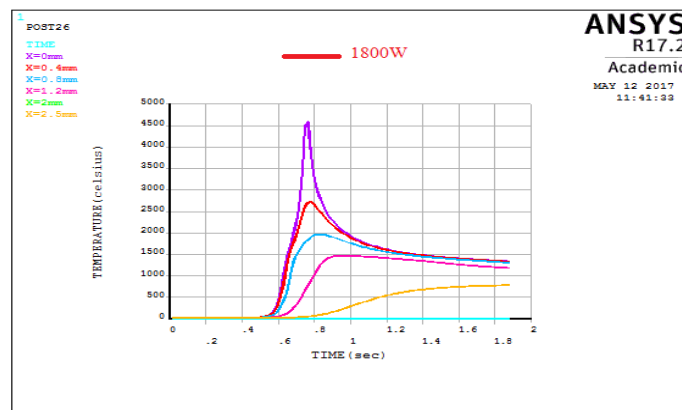


Figure 8(b): Effect of Beam Power on Temp Distribution for the Laser Parameters 800mm/min Welding Speed and 0.8mm Spot Diameter Beam Power 1800w

Figure 4 represents the effect of welding speed on the bead geometry for 1000W beam power and 0.8mm spot diameter. The figure 4 shows that there is a decrease in bead width and depth of penetration with an increase in the welding speed. The reason behind this is that there will be less time of contact between laser beam and work piece for higher welding speed and less power is transmitted to the material and hence the depth of penetration and weld bead decreases.

Figure 5 represents the effect of laser power on the temperature distribution for welding parameters 800mm/min welding speed and 0.8mm spot diameter. The value of peak temperature along the weld line increases from 3426⁰C to 4613⁰C with an increase in beam power from 1000W to 1800W. It can also be said from the figure that the melting temperature of workpiece material (1450⁰C) occurs at X=0.85mm for 1000W and at X=1.21mm for 1800W. So, the bead width will increase from 1.7mm to 2.42mm with increase in power from 1000W to 1800W at 800mm/min welding speed and 0.8mm spot diameter.

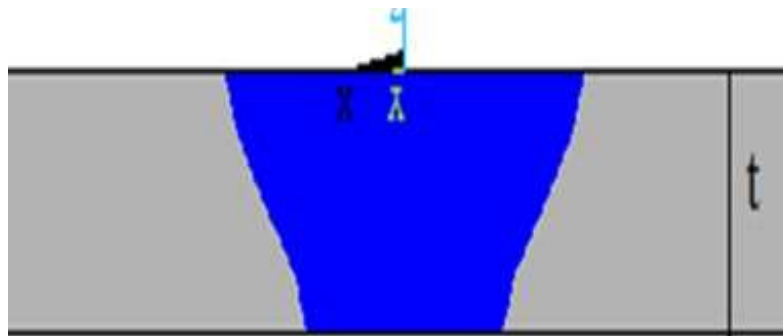


Figure 9(a): Comparison between Present Model and Published Model at 1800W Beam Power, 400mm/min Welding Speed And 0.8mm Spot Diameter Present Weld Pool Model

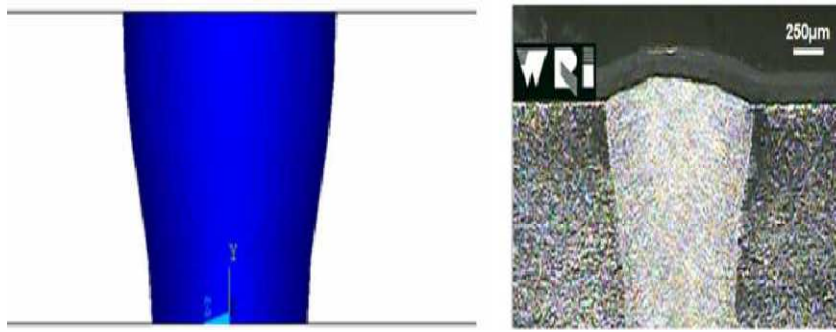


Figure 10(b): Comparison between Present Model and Published Model at 1800W Beam Power, 400mm/min Welding Speed And 0.8mm Spot Diameter Published Weld Pool Model.

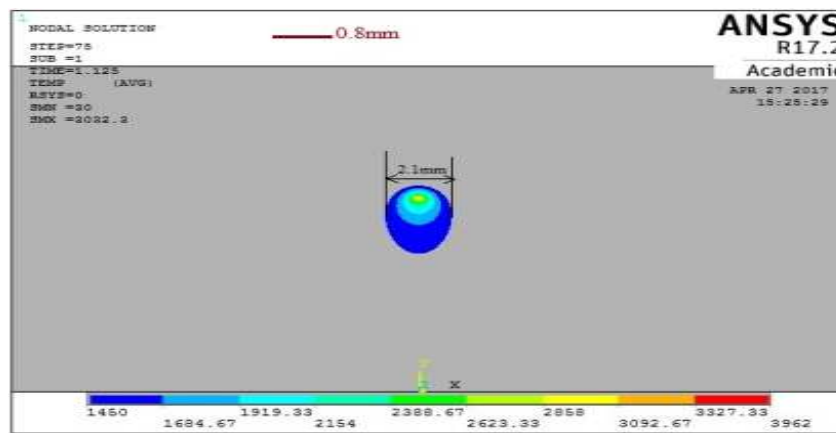


Figure 11(a): Effect of Spot Diameter on Shape and Size of Molten Pool For Welding Parameters 1400W Beam Power and 800mm/min Welding Speed Spot Diameter 0.8mm

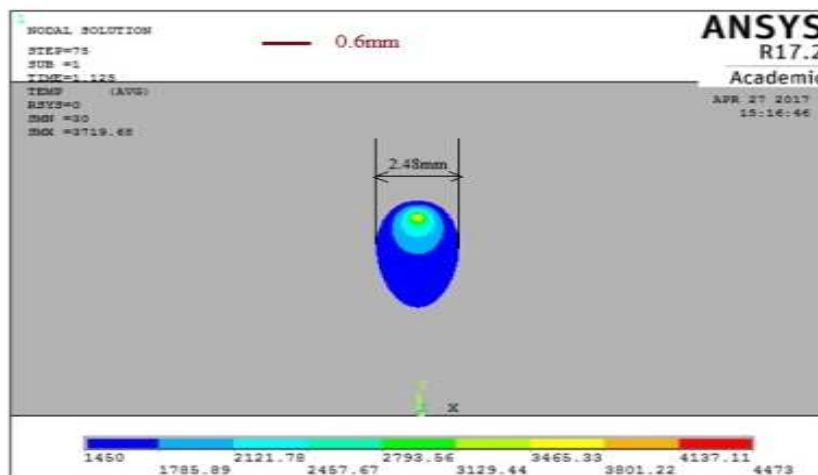


Figure 12(b): Effect of spot diameter on shape and size of molten Pool for welding parameters 1400W Beam power and 800mm/min Welding speed spot diameter 0.6mm

Figure 6 shows the comparison between the present model and published results for bead geometry at welding parameters 1800W beam power, 400mm/min welding speed and 0.8mm spot diameter. From the figure 6 it can be clearly concluded that full penetration occurs in both the cases and both are similar to the shape of bead geometry obtained

experimentally for same welding parameters. Figure 7 shows the effect of spot diameter on the shape and size of molten pool for welding parameters 1400W beam power and 800mm/min welding speed. It is clearly shown in the Figure. 7. That's the size of molten pool increases 2.1mm (bead width) to 2.48mm with a decrease in spot diameter. The reason behind this is that power density (power per unit area) will be more for lower values of spot diameter and more power is absorbed by the workpiece and hence the size of the molten pool will increase. Isotherms shown in the figure 7 starts from the melting temperature of workpiece material (1450°C) and up to the value more than the vaporization temperature in the area where laser beam irradiates. It can be seen from the figure that the isotherms are closer in front of the laser source than those are behind the source and there is some area in front of the laser source which is preheated before the power source passes through them. This occurs mainly because of the thermal conductivity of the material. Comparison between the present numerical result and published result has been shown in Table 4.

Table 4: Comparison between the Present and Published Result [3]

Beam Power	1800W
Welding speed	800mm/min
Spot diameter	0.8mm
Plate Thickness	2.5mm
Peak temperature from Present model	4886K
Peak temperature from published result	4820K

CONCLUSIONS

A three-dimensional finite element model using the commercial software ANSYS has been developed to study the Laser welding (Butt-joint) of AISI 304 stainless steel thickness 2.5mm. The process parameters such as beam power, welding speed and spot diameter and their effect on temperature profile, shape and size of molten pool and bead geometry have been discussed previously. Now, from this model the following conclusion can be made:

- The peak temperature value occurs along the weld line (4613°C) and decreases gradually as the distance increases from the weld line (nearly 1500°C at 1.2mm). Also, the peak temperature values are 4613°C and 3426°C for the beam power 1800W and 1000W respectively.
- The Size of the bead geometry increases with a decrease in welding speed and the bead width changes from 1.7mm to 2.4mm as power increases from 1000W to 1800W.
- The Size of the molten pool increases from 2.1mm to 2.48mm as the spot diameter changes from 0.8mm to 0.6mm. Isotherms are closer in front of the laser source as compare to those behind the source.
- The peak temperature values for same welding parameters are very close to each other in the present model and the published result. Also, the shapes of the bead geometry are similar in both the cases with full penetration.

REFERENCES

1. D. Rosenthal, *The Theory of Moving Sources of Heat and Its Application of Metal Treatments*. Transactions of ASME vol. 68, pp. 849-866, 1946.
2. M. R. Frewin, and D. A. Scott, *Finite element model of pulsed laser welding*, *Welding Journal-New York*- vol. 78, 15-s, 1999.
3. S. A. Tsirkas, P. Papanikos, and Kermanidis, *Numerical simulation of the laser welding process in butt-joint specimens*, *Journal of materials processing technology* vol.134, no. 1, pp. 59-69, 2003.

4. M. Guo, Han, Z. Jian, and L. J. Qang. "Dynamic simulation of the temperature field of stainless steel laser welding, *Materials & design* vol. 28, no. 1, pp. 240-245, 2007.
5. R. Spina, L. Tricarico, G. Basile, and T. Sibillano, Thermo-mechanical modeling of laser welding of AA5083 sheets, *Journal of materials processing technology* vol. 191, no. 1, pp. 215-219, 2007.
6. K. R. Balasubramanian, N. S. Shanmugam, G. Buvanashakaran, and K. Sankaranarayananamy, Numerical and experimental investigation of laser beam welding of AISI 304 stainless steel sheet, *Adv. Produc. Engineer. Manag* vol. 3, no. 2, pp. 93-105, 2008.
7. N. S. Shanmugam, G. Buvanashakaran, K. Sankaranarayananamy, and K. Manonmani. "Some studies on temperature profiles in AISI 304 stainless steel sheet during laser beam welding using FE simulation, *The International Journal of Advanced Manufacturing Technology*, vol. 43, no. 1-2, pp. 78-94, 2009.
8. E. Akman, A. Demir, T. Canel, and T. Sinmazçelik. "Laser welding of Ti6Al4V titanium alloys, *Journal of materials processing technology*, vol. 209, no. 8, pp. 3705-3713, 2009.
9. K. Kim, L. Jungkil, and C. Haeyong. "Analysis of pulsed Nd: YAG laser welding of AISI 304 steel, *Journal of Mechanical Science and Technology*, vol. 24, no. 11, pp. 2253-2259, 2010.
10. R. Wang, L. Yongping, and S. Yaowu, Numerical simulation of transient temperature field during laser keyhole welding of 304 stainless steel sheet, *Optics & Laser Technology* vol. 43, no. 4, pp. 870-873, 2011.
11. R. Bhadra, B. Pankaj, and M. R. Sankar, Effect of process parameters on thermal history of laser welding of AISI-304 stainless steel, In *5th International and 26th All India Manufacturing Technology, Design and Research Conference AIMTDR*. 2014.
12. G. Casalino, M. Mortello, N. Contuzzi, and F. M. C. Minutolo, Finite element model for laser welding of titanium, *Procedia CIRP* 33, pp. 434-439, 2015.
13. J. R. Chukkan, M. Vasudevan, S. Muthukumaran, R. Ravi Kumar, and N. Chandrasekhar, Simulation of laser butt welding of AISI 316L stainless steel sheet using various heat sources and experimental validation, *Journal of Materials Processing Technology* vol. 219, pp. 48-59, 2015.
14. K. S. Kumar, Numerical Modeling and Simulation of a Butt Joint Welding Of AISI 316L Stainless Steels Using a Pulsed Laser Beam, *Materials Today: Proceedings* vol. 2, no. 4-5, pp. 2256-2266, 2015.

